CSIRO PUBLISHING

Reproduction, Fertility and Development
https://doi.org/10.1071/RD18058

Circadian rhythms of factors involved in luteal regression are modified in p55 tumour necrosis factor receptor (TNFRp55)-deficient mice

Magali del C. de la Vega[A], *María B. Delsouc*[A], *Ivana Ponce*[B], *Vicente Ragusa*[A,B], *Sandra Vallcaneras*[A], *Ana C. Anzulovich*[B,C] *and Marilina Casais*[A,C]

[A]Laboratorio de Biología de la Reproducción, Facultad de Química, Bioquímica y Farmacia, Instituto Multidisciplinario de Investigaciones Biológicas, San Luis, Universidad Nacional de San Luis, Ejército de los Andes 950, CP D5700HHW, San Luis, Argentina.
[B]Laboratorio de Cronobiología, Facultad de Química, Bioquímica y Farmacia, Instituto Multidisciplinario de Investigaciones Biológicas, San Luis, Universidad Nacional de San Luis, Ejército de los Andes 950, CP D5700HHW, San Luis, Argentina.
[C]Corresponding authors. Emails: mcasais@unsl.edu.ar; anzulova@gmail.com

Abstract. The rhythm of factors involved in luteal regression is crucial in determining the physiological duration of the oestrous cycle. Given the role of tumour necrosis factor (TNF)-α in luteal function and circadian regulation and that most of the effects of TNF-α are mediated by p55 TNF receptor (TNFRp55), the aims of the present study were to analyse the following during the luteal regression phase in the ovary of mice: (1) whether the pattern of expression of progesterone (P4) and the enzymes involved in the synthesis and degradation of P4 is circadian and endogenous (the rhythm persists in constant conditions, (i.e., constant darkness) with a period of about 24 hours); (2) circadian oscillations in clock gene expression; (3) whether there are daily variations in the expression of key genes involved in apoptosis and antioxidant mechanisms; and (4) the consequences of TNFRp55 deficiency. P4 was found to oscillate circadianally following endogenous rhythms of clock factors. Of note, TNFRp55 deficiency modified the circadian oscillation in P4 concentrations and its enzymes involved in the synthesis and degradation of P4, probably as a consequence of changes in the circadian oscillations of brain and muscle ARNT-Like protein 1 (*Bmal1*) and Cryptochrome 1 (*Cry1*). Furthermore, TNFRp55 deficiency modified the circadian rhythms of apoptosis genes, as well as antioxidant enzymes and peroxidation levels in the ovary in dioestrus. The findings of the present study strengthen the hypothesis that dysregulation of TNF-α signalling may be a potential cause for altered circadian and menstrual cycling in some gynaecological diseases.

Additional keywords: clock, corpus luteum, ovary.

Received 9 February 2018, accepted 5 May 2018, published online 15 June 2018

Introduction

The corpus luteum (CL) is a transient endocrine structure that forms from an ovarian follicle after ovulation. The main function of the CL is the synthesis of progesterone (P4), which is necessary for the maintenance of pregnancy and regulation of the oestrous cycle. Luteal regression is essential in triggering the development of a new follicle and restarting the oestrous cycle. During the stage of dioestrus, the CL regresses, losing its capacity to produce P4 (functional regression), and undergoes structural involution (apoptosis; Bowen-Shauver and Telleria 2003).

The mammalian circadian system is a set of related neural structures organised hierarchically that provide a temporal organisation for physiological processes and behaviour (Welsh *et al.* 2010). The main components of the circadian system are a central clock, in the suprachiasmatic nucleus (SCN), and peripheral clocks (organs or tissues outside the SCN) that express circadian functioning. The SCN is trained by environmental signals and transmits the external periodicity to the peripheral clocks in the rest of the body. External environmental factors, such as light–dark cycles, temperature and food availability among others, act as circadian time cues, or *zeitgebers*, to generate endogenous rhythms with a period close to 24 h (Coogan *et al.* 2011). Light is considered the main *zeitgeber* that provides timing to the endogenous clock and assists in the process by which an individual's internal period (tau, or τ) is manipulated to match that of its environment. However, when an individual is isolated from environmental cues and kept under constant conditions (e.g. constant darkness), the persistence of rhythms is indicative of endogenous clock control. Thus, daily

oscillations observed in mice maintained under constant darkness are accurate circadian endogenous rhythms (Coogan *et al.* 2011).

In mammals, the cellular and molecular clock core includes transcriptional activators such as brain and muscle ARNT-Like protein 1 (BMAL1) and Circadian Locomotor Output Cycle Kaput (CLOCK), which heterodimerise (BMAL1:CLOCK) and bind the enhancer box (E-box), which has the DNA sequence CANNTG (where 'N' is any nucleotide), in the promoter of target clock and clock-controlled genes. The first include, although are not limited to, the period (*Per*1–3) and cryptochrome (*Cry* 1–2) genes. PER and CRY proteins undergo post-translational modifications and return to the nucleus where they act as cyclic repressors of the transcription of their own and other genes by interfering in the binding of the BMAL1:CLOCK complex to the DNA (Sellix and Menaker 2011). Interestingly, it has been reported that CL cells express the core clock genes rhythmically (Fahrenkrug *et al.* 2006).

The circadian clock seems to play a role in the temporal occurrence of steroid hormone biosynthesis (Sellix and Menaker 2011). However, there is limited information about the participation of clock in CL regression and the oestrous cycle progression.

During regression of the rat CL, inflammatory cells (including macrophages and neutrophils) and vascular endothelial cells are resident in the ovary. All these cells produce nitric oxide (NO) and reactive oxygen species (ROS), such as superoxide anion ($\cdot O^{2-}$), hydrogen peroxide (H_2O_2) and hydroxyl radical ($\cdot OH$). The CL is highly exposed to locally produced ROS due to its extensive vasculature and metabolic activity, and there is substantial evidence to indicate that ROS play an important role in CL regression (Sander *et al.* 2008). Uncontrolled ROS generation leads to increased lipid peroxidation and protein carbonylation, and causes mitochondrial dysfunction and apoptotic cell death (Zorov *et al.* 2006). Aerobic cells are equipped with antioxidant enzymes, such as catalase (CAT) and glutathione peroxidase (GPX) among others, that control ROS production and prevent the build-up of toxic levels (Al Gubory *et al.* 2012). An imbalance between pro-oxidant production and antioxidant defences plays a key role in the pathophysiology of infertility in females. It has been reported that the expression and activity of antioxidant enzymes, as well as levels of oxidative stress parameters, exhibit endogenous circadian rhythms in several mammalian tissues (Hardeland *et al.* 2003; Ponce *et al.* 2012; Navigatore-Fonzo *et al.* 2017).

It is known that CL regression is a physiological inflammatory process (Stocco *et al.* 2007). Accumulating evidence shows the presence of bidirectional links between circadian regulation and inflammatory response (Bollinger *et al.* 2010); however, the potential effect of the immune system on the molecular clock in the CL remains to be explored. A close relationship between the molecular clock and tumour necrosis factor (TNF)-α, a multifunctional hormone-like polypeptide, has been investigated in several cells and tissues (Arjona and Sarkar 2006; Cavadini *et al.* 2007). Petrzilka *et al.* (2009) showed that TNF-α reduces the expression of E-box-driven clock genes in cultured fibroblasts.

TNF-α exerts pleiotropic effects through its Type I (p55; p55 TNF receptor (TNFRp55)) and Type II (p75) receptors. At an early age, the length of the oestrous cycle is the same in TNFRp55$^{-/-}$ and wild-type female mice. However, by 6 months of age, only 40% percent of TNFRp55$^{-/-}$ female mice remained cyclic, and those that did not cycle appeared to be 'locked' into a dioestrous phase (Roby *et al.* 1999). These findings point to TNF-α as a critical regulator of luteal regression.

It has been shown TNF-α reduces gonadotrophin-induced P4 synthesis, initiates apoptosis via its TNFRp55 receptor and it is one of many cytokines involved in luteal regression (Terranova and Rice 1997; Davis and Rueda 2002). Although the mechanism(s) by which cytokines induce apoptosis vary among different cell types, it is presumed that either an increase in ROS or activation of a stress-related signalling pathways is involved (Corda *et al.* 2001; Pru *et al.* 2003).

It is unknown which of these factors, cytokines and/or ROS, have the greatest contribution to CL function. In addition, the sequence of events leading to functional and structural luteal regression at the end of the oestrous or menstrual cycle is still not clear. We wondered whether TNFRp55 deficiency affected the endogenous circadian rhythms of factors related to luteal regression in the ovary during dioestrus. To this end, we analysed possible modifications in ovarian P4 production as well as temporal changes in the expression of steroidogenic acute regulatory protein (*StAR*), 3β-hydroxysteroid dehydrogenase (*3β-HSD*) and 20α-hydroxysteroid dehydrogenase (*20α-HSD*) mRNA and 3β-HSD protein in the ovary of TNFRp55$^{-/-}$ mice in dioestrus. In addition, in order to investigate the sequence of events leading to functional and structural luteal regression, we investigated the temporal patterns of cellular clock and apoptosis-related gene expression, as well as the activity of lipid peroxidation and antioxidant enzyme, in the same experimental model.

Materials and methods

Animals

C57BL/6 wild-type (WT) mice were initially purchased from National University of La Plata (Argentina), whereas TNFRp55$^{-/-}$ mice were originally acquired from the Max von Pettenkofer Institute by the Immunopathology Laboratory (National Scientific and Technical Research Council; National University of San Luis, Argentina). Breeding colonies of both groups of mice were then established at the Animal Facility of the National University of San Luis (Argentina). Female 8-week-old nulliparous mice, either WT or TNFRp55$^{-/-}$ (knockout; KO), were maintained in a controlled environment at 22 ± 2°C under 12 h-light : 12 h-dark conditions (lights on 0700 hours; LD group) and fed irradiated food (Cargill SACI; Saladillo) and sterile water *ad libitum*. In order to analyse endogenous circadian rhythmicity, 16 mice from each group were maintained under constant darkness (dark–dark (DD) cycle) for the last 7 days before the experiment.

Mice that showed evidence of being in dioestrus (as assessed by vaginal cytology) were killed by cervical dislocation. In the present study, time is expressed as circadian time (CT). Four mice from each group were killed every 6 h starting at CT2 (where CT0 corresponds to the beginning of the 'subjective day'; that is, when the light went on) throughout a 24-h period.

Manipulation in DD conditions were performed under dim red light (<1 lx) to avoid acute effects of light. After mice had been killed, their ovaries were isolated on an ice-chilled plate, weighed and immediately placed in liquid nitrogen. All experiments were repeated at least twice.

Animals were handled following the Guidelines for the Care and Use of Laboratory Animals of the National Institutes of Health (https://www.nap.edu/catalog/5140/guide-for-the-care-and-use-of-laboratory-animals, accessed 8 February 2010). The experimental protocol was approved by the Animal Care and Use Committee of the National University of San Luis (Protocol no. B49/10).

Reagents

The chemicals and other reagents of analytical grade used in the present study were purchased from Sigma Chemical, with the exception of 1,2,6,7-[^{3}H]-progesterone (107.0 Ci mmol^{-1}), which was obtained from New England Nuclear Products.

Progesterone radioimmunoassay

P4 was measured by radioimmunoassay (RIA) in the supernatant of ovarian homogenates performed in a 1/5 (w/v) solution of 120 mM KCl and 30 mM phosphate buffer, pH 7.2. The P4 antiserum was kindly provided by R. Deis of Institute of Medicine and Experimental Biology of Cuyo (IMBECU). The P4 antiserum was produced in rabbits against P4 conjugated to bovine serum albumin (BSA) at the 11 position. The antiserum was highly specific for P4 with low cross-reactivity: <2.0% for 20α-dihydroprogesterone and deoxycorticosterone and 1.0% for other steroids (Bussmann and Deis 1979; Vallcaneras *et al.* 2016). The sensitivity of the RIA was <5ng mL^{-1} and the inter- and intraassay CVs were <10%. P4 concentrations are expressed as nanogram per microgram total protein.

RNA isolation and semiquantitative reverse transcription–polymerase chain reaction analysis

Total RNA was extracted from ovaries obtained at CT2, CT8, CT14 and CT20. All RNA isolations were performed using TRIzol reagent (Invitrogen Life Technologies) according to the manufacturer's instructions. Total RNA was then assessed for purity by measuring the absorbance at 260, 280 and 230 nm (Abs_{260}, Abs_{280} and Abs_{230} respectively) in a spectrophotometer (DU-640B; Beckman Instruments) and calculating the Abs260 : Abs280 and Abs260 : Abs230 ratios. Only samples with Abs260 : Abs280 ratios of 1.8–2.0 and Abs260 : Abs230 ratios of 2.0–2.2 were used. The integrity of the RNA samples was assessed by gel electrophoresis and GelRed staining (Biotium) and confirmed by observation of the *28S* and *18S* rRNA bands in a ratio of 2 : 1. Quantification of RNA was based on spectrophotometric analysis at 260 nm. Total RNA (2 μg) was reverse transcribed with 200 units MMLV Reverse Transcriptase (Promega) using random hexamers (Promega) in a 26 μL reaction mixture according to the manufacturer's instructions. For amplification of the reverse transcribed products, there reaction mixture consisted of 1× Green Go Taq reaction buffer, 0.2 mM dNTPs, 0.5 μM specific oligonucleotide primers (designed using Primer Express 3.0 software; Applied Biosystems) and 1.25 U Go Taq DNA polymerase (Promega) in a final volume of 50 μL. cDNA amplification was performed using a thermal cycler (MyCycler; Bio-Rad Laboratories). The polymerase chain reaction (PCR) primer sequences were as follows: *3β-HSD*, 5′-GTCTTCAGACCAGAAACCAAG-3′ (forward) and 5′-CCTTAAGGCACAAGTATGCAG-3′ (reverse); *20α-HSD*, 5′-TTCGAGCAGAACTCATGGCTA-3′ (forward) and 5′-CAACCAGGTAGAATG CCATCT-3′ (reverse); *StAR*, 5′-TTG GGCATACTCAACAACCA-3′ (forward) and 5′-GAAACACC TTGCCCACATCT-3′ (reverse); *Bmal1*, 5′-GGGAAATACGG GTGAAGTCTATGG-3′ (forward) and 5′-ATGCCTGGAAGA GTGGGATGAGTC-3′ (reverse); *Clock*, 5′-CTTCTTGGTAAC GCGAGAAAG-3′ (forward) and 5′-TCGAATCTCACTAG CATCTGACT-3′ (reverse); *Cry1*, 5′-CACTGGTTCCGAAAG GGACTC-3′ (forward) and 5′-CTGAAGCAAAAATCGCCA CCT-3′ (reverse); *Per1*, 5′-TTGGAGAGCTGCAACATTCC-3′ (forward) and 5′-TGCTGACGACGGATCTTTCTTG-3′ (reverse); *Fas*, 5′-ATGCACACTCTGCGATGAAG-3′ (forward) and 5′-CAGTGTTCACAGCCAGGAGA-3′ (reverse); Fas ligand (*FasL*), 5′-GCAGAAGGAACTGGCAGAAC-3′ (forward) and 5′-TTAATTGGGCCACACTCCTC-3′ (reverse); *Bax*, 5′-GAGCTGATCAGAACCATCAT-3′ (forward) and 5′-CATCTTCTTCCAGATGGTGA-3′ (reverse); and *Bcl-2*, 5′-G GACCATTCCACGGGAAAAC-3′ (forward) and 5′-GGCAA TTCCTGGTTCGGTTTTCA-3′ (reverse). Reaction products were electrophoresed on 2% agarose gels, visualised with GelRed (Biotium) and examined under ultraviolet transillumination. Band intensities of reverse transcription–PCR (RT-PCR) products were quantified using ImageJ software (http://rsb.info.nih.gov/ij, accessed 10 November 2016). The mRNA expression levels are expressed as the ratio of the signal intensity for the target gene relative to that of the housekeeping β-actin (*Actb*).

Western blot analysis

Samples were isolated from each group of mice at CT2, CT8, CT14 and CT20. Protein extracts were obtained from each ovary using TRIzol reagent (Invitrogen Life Technologies) according to the manufacturer's instructions. Protein concentrations were determined according to the method of Lowry *et al.* (1951). Readings were made at a wavelength of 550 nm. Aliquots containing 30 μg total protein were separated using 5–10% sodium dodecyl sulfate–polyacrylamide gel electrophoresis (SDS-PAGE) and then electrotransferred to polyvinylidene difluoride (PVDF) membranes (Millipore) at 100 V for 1 h in transfer buffer (25 mM Tris, 192 mM glycine and 20% v/v methanol, pH 8.3). Then, membranes were immersed in 5% non-fat milk in TTBS (0.2 M Tris-HCl (pH 7.6), 1.37 M NaCl, 0.5% Tween-20) for 1 h at room temperature, followed by overnight incubation at 4°C with either goat anti-3β-HSD antibody (SC-30820; Santa Cruz Biotechnology), rabbit anti-BMAL1 antibody (ab140646; Abcam) or goat anti-β-actin antibody (ACTB, C4: SC-47778; Santa Cruz Biotechnology), diluted 1 : 1000 in a 1% solution of non-fat powdered milk in TTBS. After incubation with the primary antibody, membranes were washed four times for 5 min with TTBS before being incubated with a 1 : 10 000 dilution of rabbit anti-goat IgG peroxidase-linked antibody (ZyMax Grade; Invitrogen Life Technologies) or with

a 1:10 000 dilution of horseradish peroxidase-conjugated goat anti-rabbit IgG (Jackson Immuno-Research Laboratories) in 1% milk for 1 h at room temperature. Following washing in TTBS, blots were developed using an enhanced chemiluminescence western blotting detection system using Thermo Scientific SuperSignal West Pico PLUS Chemiluminescent Substrate (Pierce Biotechnology) and exposed to X-ray films (Thermo Scientific CL-XPosure Film; Pierce Biotechnology). The mean intensity of each band was measured using National Institutes of Health ImageJ software (http://rsb.info.nih.gov/ij/, accessed 10 November 2016). 3β-HSD and BMAL1 protein levels were normalised against ACTB (endogenous control). Mean (± s.e.m.) values were calculated from three blots, each representing independent samples.

Scanning of upstream regulatory regions of putative clock-controlled genes for E-box sites

Putative clock-responsive, E-box (CACGTG) or E-box-like (CANNTG), sites were localised in regulatory regions of target genes. Thus, up to 1500 bp upstream of the translation start codon of *3β-HSD*, *20α-HSD*, *StAR*, *Fas*, *FasL*, *Bax* and *Bcl-2* genes was scanned for significant matches using MatInspector software (Genomatix; http://www.genomatix.de, accessed 12 May 2016; Cartharius *et al.* 2005). Putative P4-responsive sites were also searched for in the *Bmal1* gene regulatory region. The accession numbers for the sequences taken from the PubMed database are as follows (http://www.ncbi.nlm.nih.gov/gene, accessed 18 November 2016): *3β-HSD* (*Hsd3b1*, 3 beta-hydroxysteroid dehydrogenase/delta(5)-delta(4) isomerase type I): M58567; *20α-HSD* (*Akr1c18*, Aldo-keto reductase family 1 member C18): NM_134066; *StAR*: NM_011485; *Fas*: NC_000085.6; *FasL*: NM_010177; *Bax*: NM_007527; *Bcl-2*: NM_009741; *Bmal1*: AB086232.

Preparation of tissue extracts for antioxidant profiling

Ovary samples were homogenised in a 1/5 (w/v) solution of 120 mM KCl and 30 mM phosphate buffer, pH 7.2, at 4°C. Suspensions were centrifuged at 800*g* for 10 min at 4°C to remove nuclei and cell debris. The pellets were discarded, and antioxidant enzyme activity, thiobarbituric acid-reactive substances (TBARS) and uric acid were determined in the supernatants.

CAT and GPX activity

CAT and GPX activity was determined according to the methods of Aebi (1984) and Flohé and Günzler (1984), respectively. Briefly, CAT activity was determined by measuring the decrease in absorption at 240 nm when 100 µL of 3 mM H_2O_2 was added to a reaction medium containing 50 mM phosphate buffer, pH 7.3, and a 1 : 500 dilution of enzyme preparation. The pseudo first-order reaction constant k' ($k' = k$[CAT], where k is the catalytic rate constants) of the decrease in H_2O_2 absorption was determined, and CAT activity was calculated using $k = 4.6 \times 10^7$ M^{-1} s^{-1} and expressed in IU mg^{-1} protein. In the present study, 1 unit of CAT activity is defined as the amount of enzyme required to decompose 1 µM of H_2O_2 min^{-1}.

GPX activity was determined following NADPH oxidation at 340 nm in a reaction medium containing 0.2 mM reduced glutathione (GSH), 0.25 U mL^{-1} yeast glutathione reductase (GR), 0.5 mM tertbutyl hydroperoxide and 50 mM phosphate buffer (pH 7.2).

Uric acid levels

Uric acid was measured in 100-µL aliquots of ovary samples treated with urate oxidase, with the amount of oxygen peroxide formed quantified by a peroxidase-catalysed reaction with 4-aminophenazone and chlorophenol, which produces a coloured quinone imine product (Trinder 1969).

Lipid peroxidation

TBARS were quantified spectrophotometrically by determining malondialdehyde (MDA) levels as an indicator of TBARS according to Draper and Hadley (1990).

Statistical analysis

Time point data are expressed as the mean ± s.e.m. and pertinent curves were drawn. Time series of WT and KO groups were computed first by one-way analysis of variance (ANOVA) followed by Tukey post hoc tests for specific comparisons; two-tailed $P < 0.05$ was considered significant. When indicated, two-way ANOVA followed by Bonferroni's test was also used.

Data were fitted by the function $c + a\cos[2(t - ø)/24]$, where c is the mesor, a is the amplitude of the cosine wave, t is time in hours and ø is the phase in hours from CT0. The fitting was performed using nonlinear regression in GraphPad Prism 5.0 (GraphPad Software). The routine also estimates the standard error of the fit parameters. The standard error arises from scatter in the data and from deviations of the data from the cosine form. In addition to conventional statistics, chronobiological statistics were used to validate temporal changes as rhythms. Thus, each series was analysed using Chronos-Fit 1.06 (Zuther *et al.* 2009). Chronos-Fit is a program for the detection of rhythmic organisation in arbitrary data, which are recorded over a period in time. The program performs a rhythm analysis, which is a combination of a partial Fourier analysis and a stepwise regression technique. Although conventional partial Fourier analysis always includes all harmonics in the fitted model, the 'rhythm analysis' fits each harmonic separately and checks for significance for each using F-tests. Two-tailed $P \leq 0.05$ was taken as indicative of the presence of a rhythm with the 24-h (anticipated) period. Cosinor analysis was also performed using Cosinor 2.4 (S.E.P.T.M.R, Physiology Software Editor; www.circadian.org, accessed 2 December 2016; Refinetti *et al.* 2007). The significance of differences in mesor, amplitude and phase between the WT and KO groups was determined using Student's t-test. Data are presented as the mean ± s.e.m. and two-tailed $P < 0.05$ was considered significant.

Results

Circadian rhythms in ovaries of WT and TNFRp55-deficient mice

P4

P4 content exhibited circadian variation in the mouse ovary in dioestrus (ANOVA, $P < 0.01$; Chronos-Fit, $P < 0.001$,

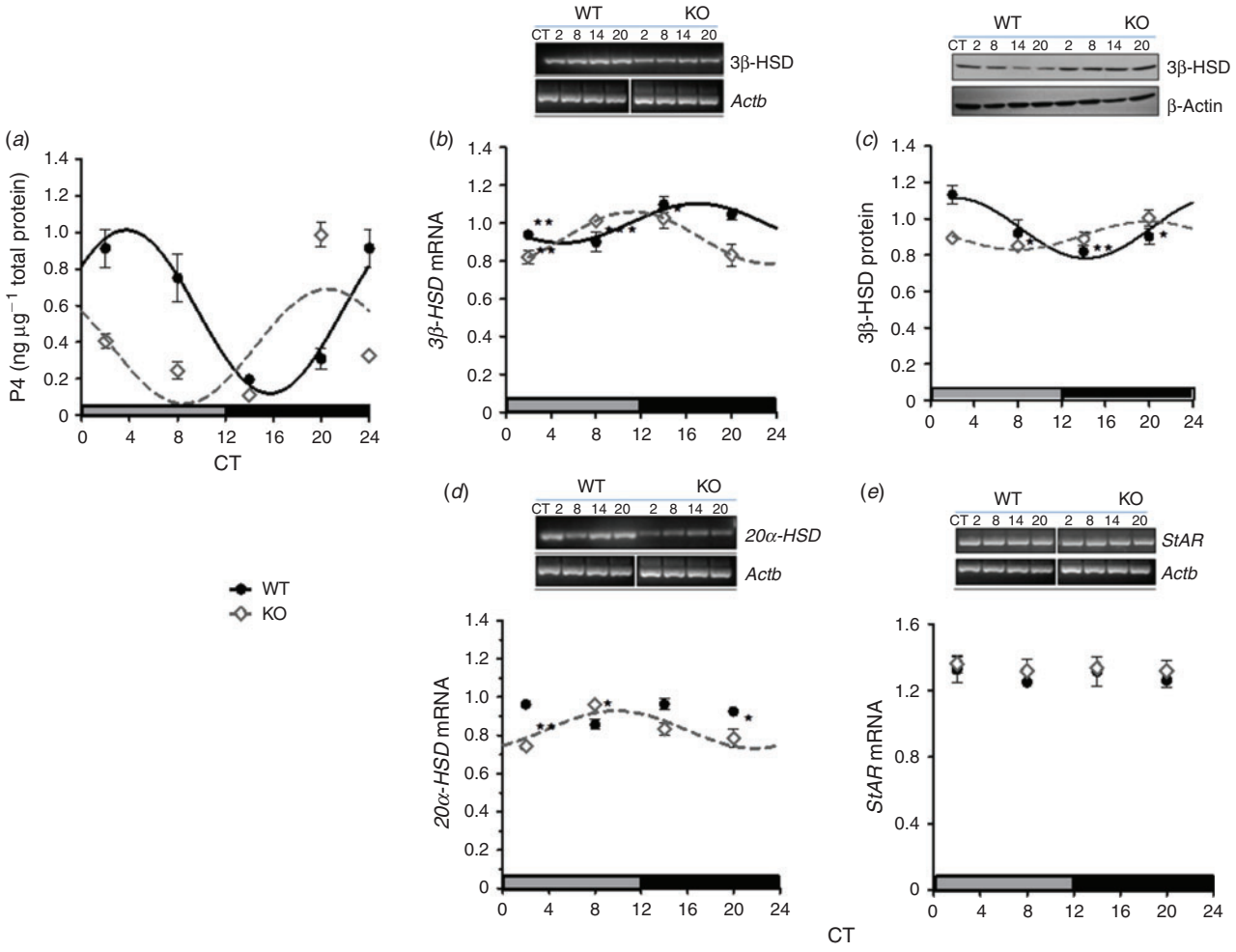

Fig. 1. Average cosinor fit for rhythmic (*a*) progesterone (P4) concentrations and (*b*, *c*) 3β-hydroxysteroid dehydrogenase (HSD) mRNA (*b*) and protein (*c*), (*d*) *20α-HSD* and (*e*) steroidogenic acute regulatory protein (*StAR*) mRNA expression in the ovary of wild-type (WT) and p55 tumour necrosis factor receptor (TNFRp55)-knockout (KO) mice. P4 concentrations were determined by radioimmunoassay, mRNA expression was determined by reverse transcription–polymerase chain reaction and 3β-HSD protein levels were determined by western blot analysis at circadian times (CT) 2, CT8, CT14 and CT20, where CT0 corresponds to the beginning of the 'subjective day'; that is, when the light went on. Horizontal bars represent the distribution of the subjective day (grey) and night (black) phases of a 24-h period. Data are the mean ± s.e.m. ($n = 5$ samples at a particular CT). Data were fitted to a cosine curve using a non-linear regression program of GraphPad Prism 5.0. The statistical significance of daily variations in P4 concentrations was analysed by one-way ANOVA, followed by Tukey's test. *$P < 0.05$, **$P < 0.01$, ***$P < 0.001$ for comparisons of the mean value at each time point with the maximum value of each curve. From the Chronos-Fit analysis, $P \leq 0.05$ indicates detection of a rhythm. *Actb*, β-actin.

85.4% rhythm; Fig. 1*a*). The cosinor (Refinetti *et al.* 2007) and Chronos-Fit (Zuther *et al.* 2009) analyses revealed P4 content in the ovary is maximal (acrophase) at CT 04:03 ± 00:10 (Fig. 1*a*; Table 1). Interestingly, TNFRp55 deficiency reduced P4 rhythmicity (Chronos-Fit 49.66% rhythm) and resulted in a phase delay in P4 circadian oscillations in mouse ovaries in dioestrus II (ANOVA, $P < 0.001$; Chronos-Fit, $P < 0.05$), with the rhythm's acrophase occurring at CT 21:15 ± 00:04 (*t*-test, $P < 0.001$; Fig. 1*a*; Table 1).

Enzymes involved in the synthesis and degradation of P4

The observation of P4 circadian rhythms in the ovaries of mice in dioestrus led us to analyse the temporal expression of the enzymes involved in the synthesis and degradation of P4 (3β-HSD, 20α-HSD and StAR) in the same samples. There were significant variations in 3β-HSD mRNA (ANOVA, $P < 0.05$; Chronos-Fit, $P < 0.001$, 81.1% rhythm) and protein (ANOVA, $P < 0.01$; Chronos-Fit $P < 0.01$, 67.9% rhythm) levels throughout the day in the mouse ovary, with maximum mRNA and protein levels occurring at CT 16:45 ± 00:05 and 02:28 ± 00:58 respectively. However, there was no variation in *20α-HSD* and *StAR* transcript levels during the same period (Fig. 1*b*–*e*).

Interestingly, in KO mice, *3β-HSD* transcript levels continued oscillating (ANOVA, $P < 0.05$; Chronos-Fit, $P < 0.001$, 81.5% rhythm), but TNFRp55 deficiency advanced the phase (from CT 16:45 ± 00:05 to 11:07 ± 00:31) and reduced the mesor (from 1.00 ± 0.01 to 0.92 ± 0.01) of *3β-HSD* circadian expression (Fig. 1*b*; Table 1). Although 3β-HSD protein levels

Table 1. Circadian rhythm parameters of progesterone (P4) levels, 3β-hydroxysteroid dehydrogenase (*3β-HSD*) and 20α-hydroxysteroid dehydrogenase (*20α-HSD*) mRNA and 3β-HSD protein expression in ovaries of wild-type (WT) and p55 tumour necrosis factor receptor-deficient (knockout; KO) mice

Data are the mean ± s.e.m. *P*-values for comparisons of WT and KO groups were calculated using Student's *t*-test ($n = 5$). Phase, in hours, is time from CT0, which corresponds to the beginning of the 'subjective day'; that is, when the light went on. NA, not applicable

	Mesor			Amplitude			Phase		
	WT	KO	*P*-value	WT	KO	*P*-value	WT	KO	*P*-value
P4 (ng/μg total protein)	0.51 ± 0.01	0.42 ± 0.04	NS	0.37 ± 0.01	NA	NA	04:03 ± 00:10	21:15 ± 00:04	<0.001
3β-HSD mRNA (relative units)	1.00 ± 0.01	0.92 ± 0.01	<0.05	0.11 ± 0.00	0.14 ± 0.01	NS	16:45 ± 00:05	11:07 ± 00:31	<0.001
3β-HSD protein (relative units)	0.94 ± 0.01	0.91 ± 0.00	NS	0.17 ± 0.02	0.09 ± 0.03	NS	02:28 ± 00:58	19:16 ± 01:42	<0.001
20α-HSD mRNA (relative units)	0.93 ± 0.01	0.83 ± 0.02	<0.05	NA	0.10 ± 0.02	NA	NA	10:00 ± 00:54	NA

also varied significantly throughout the 24-h period in ovaries of TNFRp55-deficient mice (ANOVA, $P < 0.05$; Chronos-Fit, $P < 0.05$), TNFRp55 deficiency reduced rhythmicity (Chronos-Fit 57.2% rhythm) and delayed the acrophase of the 3β-HSD rhythm to CT 19:16 ± 01:42, without affecting the rhythm's mesor or amplitude (Fig. 1*c*; Table 1).

In addition, TNFRp55 deficiency induced a circadian oscillation of *20α-HSD* mRNA levels (ANOVA, $P < 0.05$; Chronos-Fit, $P < 0.05$, 56.8% rhythm), which was maximal at CT 10:00 ± 00:54 (Fig. 1*d*; Table 1).

Apoptotic genes

Rhythmic expression was found for extrinsic apoptotic factors *Fas* and *FasL*, peaking at CT 18:07 ± 00:26 (ANOVA, $P < 0.05$; Chronos-fit, $P < 0.05$, 61.24% rhythm) and CT 18:22 ± 01:03 (ANOVA, $P < 0.05$; Chronos-fit $P < 0.05$, 51.92% rhythm) respectively in the ovaries of WT mice in dioestrus. TNFRp55 deficiency abolished the circadian oscillation in *Fas* and *FasL* expression (Fig. 2*a*, *b*; Table 2).

Intrinsic proapoptotic *Bax* and antiapoptotic *Bcl-2* gene expression also exhibited circadian oscillation in WT mice ovaries, with peaks at CT 13:49 ± 00:55 (ANOVA, $P < 0.01$; Chronos-Fit, $P < 0.01$, 70.31% rhythm) and CT 16:10 ± 00:20 (ANOVA, $P < 0.05$; Chronos-Fit, $P < 0.05$, 58.93% rhythm) respectively. In this case, TNFRp55 deficiency had a differential effect on the temporal expression patterns of these genes, delaying the acrophase of the circadian rhythm of *Bax* from CT 13:49 ± 00:55 to 19:12 ± 00:26 (ANOVA, $P < 0.05$; Chronos-Fit, $P < 0.01$, 68.9% rhythm), but advancing the peak of circadian rhythm of *Bcl-2* from CT 16:10 ± 00:20 to 09:05 ± 00:20 (ANOVA, $P < 0.01$; Chronos-Fit, $P < 0.01$, 64.56% rhythm; Fig. 2*c*, *d*; Table 2).

Putative clock-responsive sites in regulatory regions of the enzymes involved in the synthesis and degradation of P4 and apoptosis genes

Circadian rhythms in the expression of the enzymes involved in the synthesis and degradation of P4 and apoptosis genes led us to look for putative clock-responsive binding sites in regulatory regions of the *3β-HSD*, *20α-HSD*, *StAR*, *Fas*, *FasL*, *Bax* and *Bcl-2* genes. Thus, a 1500-bp region upstream of the translation start codon was scanned using the MatInspector (Cartharius *et al.* 2005). Five and four E-box-like (CANNTG) motifs were found in the 5 regulatory region of the *3β-HSD* and *StAR* genes respectively. However, no clock-responsive site was found in the regulatory region of *20α-HSD*. Conversely, bioinformatic analysis revealed one and two perfect CACGTG E-box sites in the gene promoter regions of *Fas* and *Bax* respectively. In addition, two E-box-like sites were found in each of these genes. Similar analysis showed five and four E-box-like motifs within 1500 bp upstream of the translation start codon of the *FasL* and *Bcl2* genes (Fig. 3).

Circadian rhythms of clock gene expression in ovaries of WT and TNFRp55-deficient mice

After finding putative clock-responsive sites in the 5′ regulatory region of the enzymes involved in the synthesis and degradation of P4 and apoptosis-related genes, we continued analysing the temporal variation of clock gene expression throughout a 24-h period in ovaries of mice in dioestrus maintained under constant darkness. In these mice, Bmal1 gene and protein expression is rhythmic, circadian and endogenously driven in the mouse ovary in dioestrus, peaking at CT 16:36 ± 00:24 (ANOVA, $P < 0.01$; Chronos-Fit $P < 0.05$, 63.7% rhythm) and CT 12:10 ± 01:34 (ANOVA, $P < 0.05$; Chronos-Fit, $P < 0.05$, 60.09% rhythm) respectively. In the case of *Cry1* expression, although arrhythmic, transcript levels varied significantly throughout the 24-h period (ANOVA, $P < 0.01$), with the highest levels occurring at CT14 (Fig. 4*e*). In contrast, *Clock* and *Per1* mRNA levels did not vary significantly throughout the 24-h period in mouse ovaries.

The expression of circadian clock genes was differentially affected in TNFRp55-deficient mice. TNFRp55 deficiency advanced the acrophase of the circadian rhythm of Bma1 mRNA and protein from CT 16:36 ± 00:24 to 07:40 ± 00:39 (*t*-test, $P < 0.001$) and from CT 12:10 ± 10:34 to 05:30 ± 00:55 (*t*-test, $P < 0.05$) respectively. Conversely, arrhythmic *Cry1* gene in WT mice was rhythmic and circadian in TNFRp55-deficient mice in dioestrus (ANOVA, $P < 0.01$; Chronos-Fit, $P < 0.05$, 51.5% rhythm), peaking at CT 02:03 ± 00:18 (Fig. 4*a–e*; Table 3). TNFRp55 deficiency did not affect *Clock* or *Per1* expression.

Putative P4-responsive sites in the regulatory region of Bmal1

Given evidence of the endocrine regulation of clock gene expression (Trinder 1969), we continued analysing the

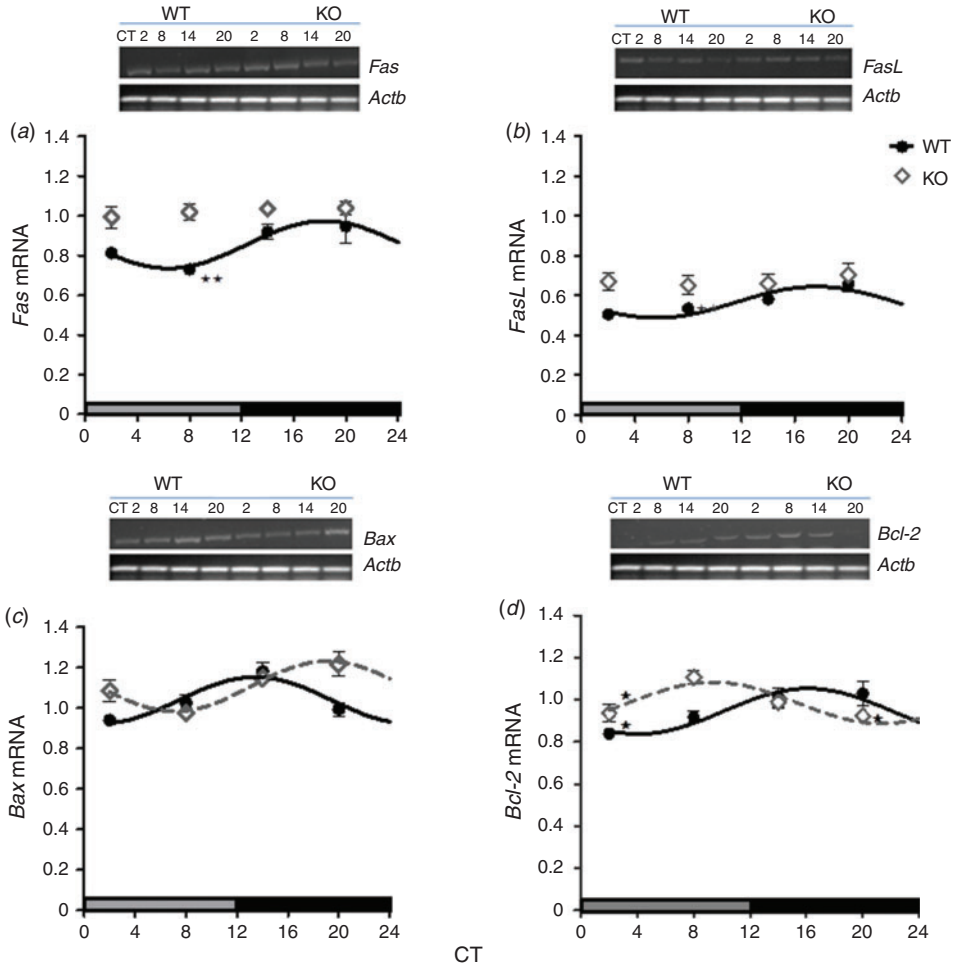

Fig. 2. Average cosinor fit for (*a*) *Fas*, (*b*) Fas ligand (*FasL*), (*c*) *Bax* and (*d*) *Bcl-2* mRNA expression in the ovary of wild-type (WT) and p55 tumour necrosis factor receptor (TNFRp55)-knockout (KO) mice. Expression of apoptosis-related genes was determined by reverse transcription–polymerase chain reaction in ovary samples obtained at circadian times (CT) 2, CT8, CT14 and CT20, where CT0 corresponds to the beginning of the 'subjective day'; that is, when the light went on. Horizontal bars represent the distribution of subjective day (grey) and night (black) phases of a 24-h period. Curves represent normalised mRNA levels versus CT. Data are the mean ± s.e.m. ($n = 4$ samples at a particular CT). Data were fitted to a cosine curve using a non-linear regression program of GraphPad Prism 5.0. The statistical significance of the temporal variation in mRNA expression was analysed by one-way ANOVA, followed by Tukey's test. *$P < 0.05$, **$P < 0.01$, ***$P < 0.001$ for comparisons of the mean value at each time point with the maximum value of each curve. From the Chronos-Fit analysis, $P \leq 0.05$ indicates detection of a rhythm. *Actb*, β-actin.

Table 2. Circadian rhythm parameters of *Fas*, Fas ligand (*FasL*), *Bax* and *Bcl-2* mRNA expression in ovaries of wild-type (WT) and p55 tumour necrosis factor receptor-deficient (knockout; KO) mice

Data are the mean ± s.e.m. *P*-values for comparisons of WT and KO groups were calculated using Student's *t*-test ($n = 5$). Phase, in hours, is time from CT0, which corresponds to the beginning of the 'subjective day'; that is, when the light went on. NA, not applicable

	Mesor			Amplitude			Phase		
	WT	KO	*P*-value	WT	KO	*P*-value	WT	KO	*P*-value
Fas mRNA (relative units)	0.85 ± 0.03	1.02 ± 0.04	<0.05	0.12 ± 0.04	NA	–	18:07 ± 00:26	NA	–
FasL mRNA (relative units)	0.57 ± 0.02	0.671 ± 0.002	<0.01	0.08 ± 0.02	NA	–	18:22 ± 01:03	NA	–
Bax mRNA (relative units)	1.03 ± 0.01	1.10 ± 0.01	<0.05	0.13 ± 0.02	0.13 ± 0.02	NS	13:49 ± 00:55	19:12 ± 00:26	<0.01
Bcl-2 mRNA (relative units)	0.95 ± 0.04	0.98 ± 0.03	NS	0.10 ± 0.02	0.096 ± 0.01	NS	16:10 ± 00:20	09:05 ± 00:20	<0.0001

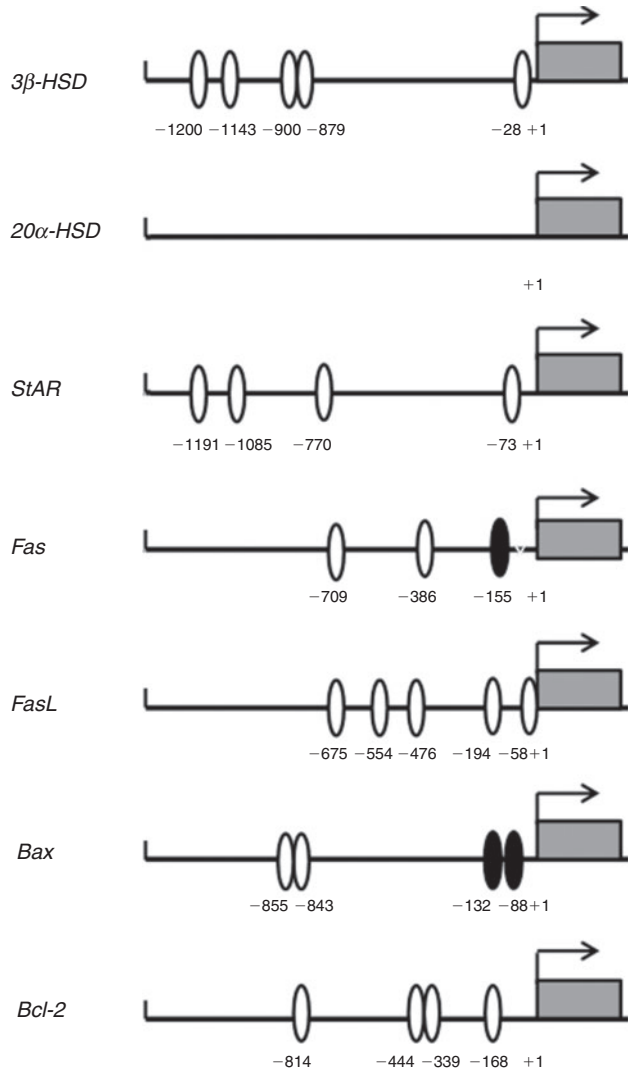

Fig. 3. Schematic representation of enhancer box (E-box) sites on the 5′ regulatory region of 3β-hydroxysteroid dehydrogenase (HSD), *20α-HSD*, steroidogenic acute regulatory protein (*StAR*), *Fas*, Fas ligand (*FasL*), *Bax* and *Bcl-2* genes. The accession numbers for the sequences taken from the PubMed database (http://www.ncbi.nlm.nih.gov/gene, accessed 18 November 2016) are as follows: *3β-HSD* (*Hsd3b1*), M58567; *20α-HSD* Akr1c18, NM_134066; *StAR*, NM_011485; *FasL*, NM_010177; *Fas*, NM_007987; *Bax*, NM_007527; *Bcl-2*, NM_009741. Arrows indicate the first translation codon, grey boxes represent exons, black ovals are perfect E-boxes (CACGTG) and white ovals are E-box-like (CANNTG) sites. Negative numbers indicate regulatory site positions relative to the start of translation (+1).

regulatory region of *Bmal1*. To this end, a 1500-bp segment upstream of the translation start codon was scanned using MatInspector software (Cartharius *et al.* 2005), revealing a glucocorticoid-responsive element (GRE) at position −46 bp in the *Bmal1* gene promoter (data not shown).

Circadian oscillation of enzyme and non-enzyme antioxidants in ovaries WT and TNFRp55-deficient mice

Both CAT and GPX activity exhibited circadian rhythms in the mouse ovary in dioestrus (ANOVA, $P < 0.05$; Chronos-Fit, $P < 0.05$, 77.08% rhythm and 62.05% rhythm respectively), with the acrophase of the CAT rhythm occurring at CT 07:03 ± 00:02 and maximal GPX activity occurring at CT 09:07 ± 0:03 (Fig. 5*a*, *b*; Table 4). In contrast, uric acid, a non-enzyme antioxidant, did not exhibit circadian variations in the mouse ovary (Fig. 5*c*).

TNFRp55 deficiency reduced the mesor of the CAT rhythm (1.71 ± 0.03 vs 0.95 ± 0.05 respectively; $P < 0.001$; Table 4) and introduced a phase delay in the acrophase from CT 07:03 ± 00:02 to 23:16 ± 00:02 ($P < 0.001$; Table 4). In contrast, no changes were observed in the mesor, amplitude or acrophase of the GPX activity rhythm in ovaries of KO mice in dioestrus. However, a significant increase in GPX activity was observed at CT 8:00 in the ovary KO mice (two-way ANOVA, $P < 0.01$; Fig. 5*b*).

Uric acid levels continue to be arrhythmic in the ovary of TNFRp55-deficient mice, although they were significantly increased at CT 14:00 compared with levels at the same time point in WT mice (two-way ANOVA, $P < 0.05$; Fig. 5*c*).

Circadian oscillation of lipid peroxidation in ovaries of WT and TNFRp55-deficient mice

Lipid peroxidation exhibited circadian variation in ovaries of WT mice in dioestrus, peaking at CT 19:19 ± 01:10 (ANOVA, $P < 0.05$; Chronos-Fit, $P < 0.05$, 50.71% rhythm; Fig. 5*d*; Table 4). TBARS levels continued oscillating in ovaries of TNFRp55-deficient mice (ANOVA, $P < 0.05$; Chronos-Fit, $P < 0.05$, 53.92% rhythm), but TNFRp55 deficiency increased the mesor and amplitude of the lipid peroxidation rhythm (*t*-test, $P < 0.05$) and advanced the phase of the rhythm's acrophase from CT 19:19 ± 01:10 to 10:51 ± 04:59 (*t*-test $P < 0.01$; Fig. 5*d*; Table 4).

Discussion

In the present study we have shown, to the best of our knowledge for the first time, participation of the endogenous cellular clock in the temporal organisation of functional and structural luteal regression. In addition, we demonstrated that TNFRp55 is crucial for the sequence of events and temporal relationship between factors that trigger luteal regression.

It is known that P4 levels oscillate rhythmically throughout the oestrous cycle and on a daily basis (Smith *et al.* 1975; Zhang *et al.* 2017). In accordance with the findings of Smith *et al.* (1975), in the present study we observed that P4 levels exhibit circadian oscillation during dioestrus II in the mouse ovary, with maximum concentrations occurring at the beginning of the subjective day. This observation led us to analyse the temporal expression of the enzymes involved in the synthesis and degradation of P4, namely 3β-HSD, 20α-HSD and StAR. Only expression of the 3β-HSD enzyme, involved in the synthesis of P4, exhibited a circadian rhythm during dioestrus II in the mouse ovary. Specifically, *3β-HSD* mRNA levels peaked at CT 16:45 ± 00:05, whereas protein levels were maximal at CT 02:28 ± 00:58, preceding, as expected, the P4 diurnal peak. These results differ from those reported by Boden *et al.* (2010), who did not find a circadian rhythm for P4 during dioestrus II. This difference could rise from the lighting

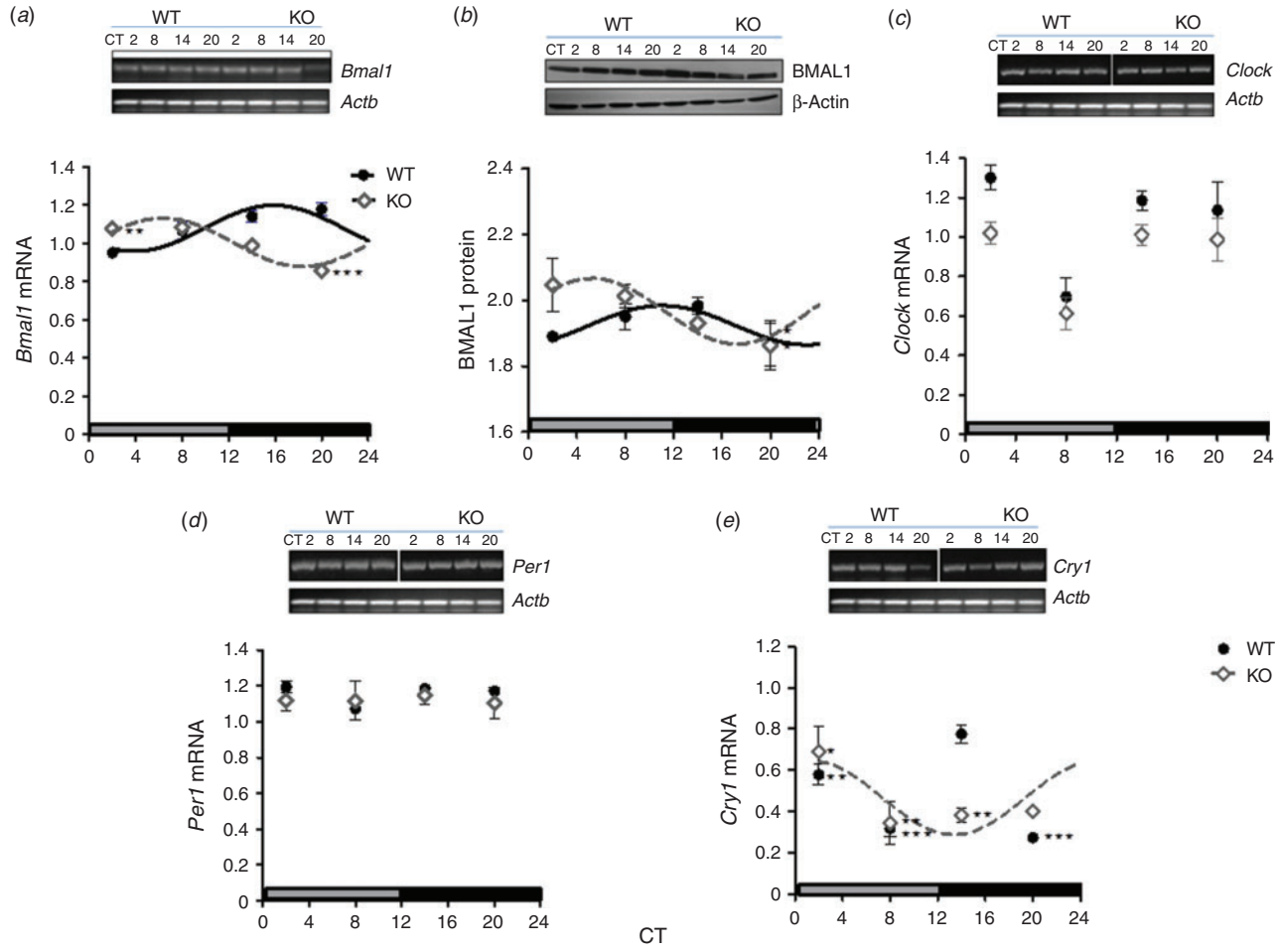

Fig. 4. Average cosinor fit for rhythmic (*a, b*) Brain and muscle ARNT-Like protein 1 (Bmal1) mRNA (*a*) and protein (*b*), (*c*) *Clock*, (*d*) period 1 (*Per1*) and (*e*) Cryptochrome 1 (*Cry1*) mRNA expression in the ovary of wild-type (WT) and p55 tumour necrosis factor receptor (TNFRp55)-knockout (KO) mice maintained under constant darkness. Clock gene expression was determined by reverse transcription–polymerase chain reaction and BMAL1 protein levels were determined by western blot analysis in ovary samples obtained at circadian times circadian times (CT) 2, CT8, CT14 and CT20, where CT0 corresponds to the beginning of the 'subjective day'; that is, when the light went on**.** Horizontal bars represent the distribution of subjective day (grey) and night (black) phases of a 24-h period. Data are the mean ± s.e.m. ($n = 4$ samples at a particular CT). The data were fitted to a cosine curve using the non-linear regression program of GraphPad Prism 5.0. The statistical significance of the circadian variation of clock genes expression was analysed by one-way ANOVA, followed by Tukey's test. $^{*}P < 0.05$, $^{**}P < 0.01$, $^{***}P < 0.001$ for comparisons of the mean value at each time point with the maximum value of each curve. From the Chronos-Fit analysis, $P \leq 0.05$ indicates detection of a rhythm. *Actb*, β-actin.

Table 3. Circadian rhythm parameters for Brain and muscle ARNT-Like protein 1 (*Bmal1)* and Cryptochrome 1 (*Cry1)* mRNA expression and BMAL1 protein levels in ovaries of wild-type (WT) and p55 tumour necrosis factor receptor-deficient (knockout; KO) mice

Data are the mean ± s.e.m. *P*-values for comparisons of WT and KO groups were calculated using Student's *t*-test ($n = 5$). Phase, in hours, is time from CT0, which corresponds to the beginning of the 'subjective day'; that is, when the light went on. NA, not applicable

	Mesor			Amplitude			Phase		
	WT	KO	*P*-value	WT	KO	*P*-value	WT	KO	*P*-value
Bmal1 mRNA (relative units)	1.11 ± 0.03	0.98 ± 0.01	NS	0.09 ± 0.01	0.14 ± 0.03	NS	16:36 ± 00:24	07:40 ± 00:39	<0.001
BMAL1 protein (relative units)	0.192± 0.001	0.196 ± 0.003	NS	0.007 ± 0.002	0.009 ± 0.001	NS	12:10 ± 01:34	05:30 ± 00:55	<0.05
C*ry1* mRNA (relative units)	0.44 ± 0.02	0.46 ± 0.04	NS	NA	0.17 ± 0.02	NA	NA	02:03 ± 00:18	NA

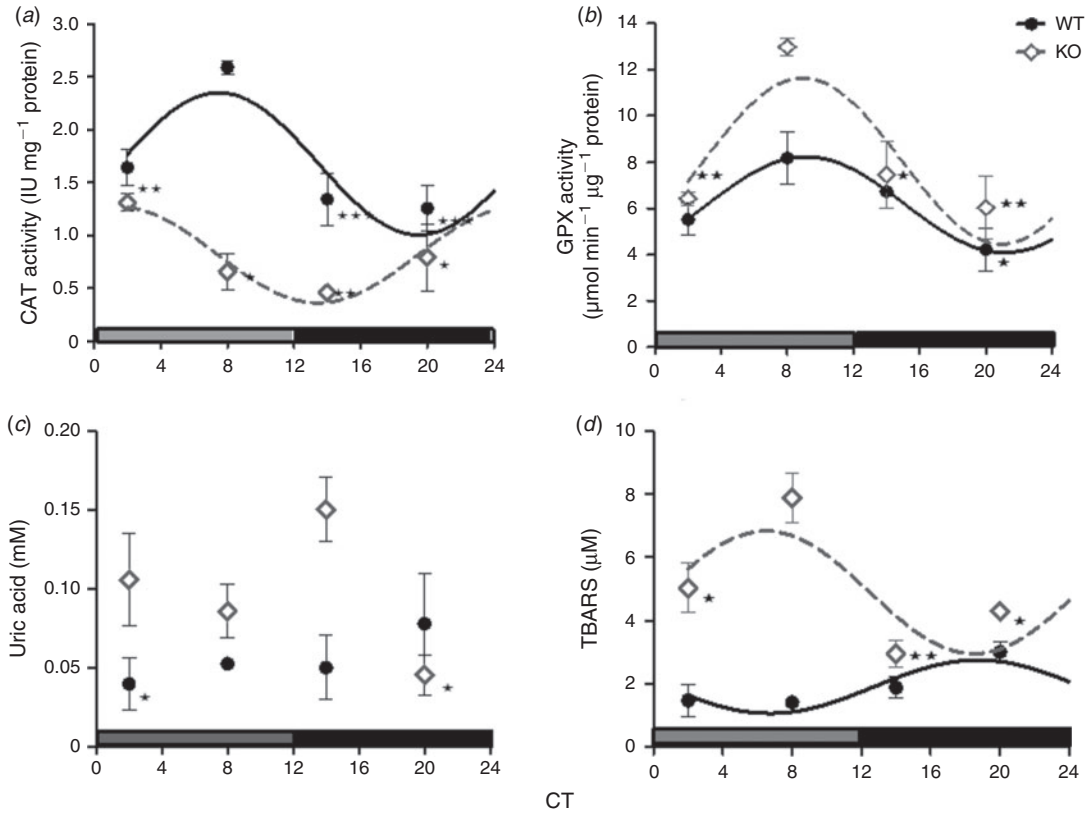

Fig. 5. Average cosinor fit for (*a*) catalase (CAT) and (*b*) glutathione peroxidase (GPX) activity, (*c*) uric acid and (*d*) lipid peroxidation, as indicated by thiobarbituric acid-reactive substances (TBARS) levels, in the ovary of wild-type (WT) and p55 tumour necrosis factor receptor (TNFRp55)-knockout (KO) mice. CAT and GPX activities were determined by kinetic assays, uric acid and TBARS concentrations were determined spectrophotometrically in ovary samples obtained at circadian times circadian times (CT) 2, CT8, CT14 and CT20, where CT0 corresponds to the beginning of the 'subjective day'; that is, when the light went on. Horizontal bars represent the distribution of subjective day (grey) and night (black) phases of a 24-h period. Curves represent normalised protein levels versus CT. Data are the mean ± s.e.m. ($n = 4$ samples at a particular CT). The data were fitted to a cosine curve using the non-linear regression program of GraphPad Prism 5.0. The statistical significance of the temporal variation of enzyme expression was analysed by one- and two-way ANOVA, followed by Tukey or Bonferroni tests respectively. $^{*}P < 0.05$, $^{**}P < 0.01$, $^{***}P < 0.001$ for comparisons of the mean value at each time point with the maximum value of each curve. From the Chronos-Fit analysis, $P \leq 0.05$ indicates detection of a rhythm.

Table 4. Circadian rhythm parameters for catalase (CAT) and glutathione peroxidase (GPX) activity and lipid peroxidation in ovaries of wild-type (WT) and p55 tumour necrosis factor receptor-deficient (knockout; KO) mice

Lipid peroxidation was determined as thiobarbituric acid-reactive substances (TBARS). Data are the mean ± s.e.m. *P*-values for comparisons of WT and KO groups were calculated using Student's *t*-test ($n = 5$). Phase, in hours, is time from CT0, which corresponds to the beginning of the 'subjective day'; that is, when the light went on.

	Mesor			Amplitude			Phase		
	WT	KO	*P*-value	WT	KO	*P*-value	WT	KO	*P*-value
CAT (IU/mg prot)	1.71 ± 0.03	0.95 ± 0.05	0.0002	0.69 ± 0.07	0.57 ± 0.07	NS	07:03 ± 00:02	23:16 ± 00:02	<0.001
GPX (µM/min/µg prot)	0.62 ± 0.07	0.82 ± 0.06	NS	0.21 ± 0.07	0.36 ± 0.07	NS	09:07 ± 00:03	08:45 ± 00:05	NS
TBARS (µM/L)	1.95 ± 0.29	4.62 ± 0.63	<0.05	0.90 ± 0.10	2.28 ± 0.46	<0.05	19:19 ± 01:10	10:51 ± 04:59	<0.01

conditions in the different studies. In the present study, experiments were conducted in mice kept under constant darkness (DD), because one of the study aims was to analyse the endogenous characteristics that define clock-controlled circadian rhythms, whereas the study of Boden *et al.* (2010) was performed under a light-dark cycle (12 h-12 h). Thus, the apparent discrepancy regarding a circadian rhythm for 3β-HSD expression between the present study and that of Boden *et al.*

(2010) may be explained by a light masking effect, similar to that described by Redlin (2001) on melatonin synthesis.

Conversely, we observed no variations in either *20α-HSD* or *StAR* transcript levels over a 24-h period in mouse ovary, even in mice kept in constant darkness. These findings were also reported by Boden *et al.* (2010) in rats maintained under a light-dark cycle (12 h-12 h) during dioestrus. However, Nakao *et al.* (2007) found that StAR is expressed in a circadian manner in quail preovulatory ovarian follicles.

Proapoptotic and antiapoptotic factors have been implicated in structural luteal regression. To elucidate the temporal sequence of events that, at any given time, triggers luteal regression, we analysed the time-related variations in *Fas*, *FasL*, *Bax* and *Bcl-2* expression over a 24-h period in the ovaries of mice in dioestrus II. Interestingly, we describe, for the first time, circadian expression patterns of extrinsic, as well as intrinsic, apoptotic and antiapoptotic factors, in the mouse ovary in dioestrus. Even though we did not find any reports of daily variations in apoptosis-related factors in the ovary, rhythms have been reported for BAX and BCL-2 protein expression in mouse bone marrow by Granda *et al.* (2005).

Tasaki *et al.* (2013) reported that the mRNA expression of *Fas* and *caspase 3* does not vary over a 24-h period in uterine endometrial stromal cells of pregnant rats; however, in that study, transcript levels of both *Fas* and *caspase 3* increased after *Bmal1* gene silencing. In the present study, maximum *Bax* mRNA expression in WT mice was seen at the beginning of active phase, concurrent (as expected) with the lowest P4 concentrations. Expression of the extrinsic proapoptotic factors *Fas* and *FasL* peaked in the middle of the night following Bax maximal expression. Conversely, antiapoptotic *Bcl-2* expression was maximal at CT 16:10 ± 00:20.

The persistence of rhythmic expression of *3β-HSD*, *Fas*, *FasL*, *Bax* and *Bcl-2* under DD conditions led us to think those genes could be under endogenous clock control. Thus, we first analysed the regulatory regions of the rhythmically expressed *3β-HSD*, *Fas*, *FasL*, *Bax* and *Bcl-2* genes, as well as the arrhythmically expressed *StAR* and *20α-HSD* genes, in search of putative clock-responsive binding sites. Perfect E-box sites were found in the promoter regions for the *Bax* and *Fas* genes, and E-box-like motifs were found in the regulatory regions of the *3β-HSD*, *StAR*, *Fas*, *FasL*, *Bax* and *Bcl-2* genes (Fig. 3).

Having determined the presence of clock-responsive sites in the regulatory regions of the rhythmically expressed genes, we continued analysing the temporal expression of molecular clock factors *Bmal1*, *Clock*, *Per1* and *Cry1*. Interestingly, both Bmal1 mRNA and protein levels were found to oscillate rhythmically in the mouse ovary during dioestrus II. However, *Clock, Per1* and *Cry1* gene expression was arrhythmic, although *Cry1* mRNA levels varied significantly throughout a day in the same tissue. Our results are similar to those of Nakamura *et al.* (2010) and Boden *et al.* (2010), who reported rhythmic variation in *Bmal1* mRNA and arrhythmic expression of *Clock* and *Per1* genes in the ovary of rats in dioestrus under a light-dark cycle (12 h-12 h). Also the same lines, Chen et al. (2013) showed a robust circadian *Bmal1* mRNA rhythm, but flatter *Per1* oscillation and arrhythmic *Clock* gene expression in mouse luteinised granulosa cells.

Circadian *Bmal1* rhythms in the ovary could be affected by steroid and LH and FSH hormones (Boden *et al.* 2010). Nakamura *et al.* (2010) demonstrated that the timing of the circadian clock in reproductive tissues is affected by the oestrous cycle and suggested that fluctuating steroid hormone levels may be responsible for this, at least in part, through a direct effect on the timing of *clock* gene expression. In the present study, the peak of the *Bmal1* mRNA rhythm occurred during the first half of the subjective night, in antiphase with the ovarian P4 oscillation. Sugino *et al.* (1997) provided evidence that despite the absence of specific P4 receptors in the rat CL, P4 can act through glucocorticoid receptors to downregulate 20α-HSD expression. Interestingly, we found a GRE site in the promoter of the *Bmal1* gene, which may indicate that Bmal1 expression can be downregulated by P4 at the beginning of the subjective day.

Given the presence of putative clock-responsive sites in the regulatory regions of the *Bax*, *Fas* and *FasL* genes and that the peak in the BMAL1 rhythm precedes the acrophase of those genes' circadian expression, we suggest that the endogenous clock may participate in triggering luteal regression via apoptotic pathways. However, such participation would require a suitable cellular redox microenvironment, at the appropriate time.

Considering that endogenous cellular clock activity and CL function and integrity depend on the local cellular redox state, we continued analysing the circadian oscillation of enzyme and non-enzyme antioxidants, as well as a parameter of oxidative stress (i.e. lipid peroxidation), in the mouse ovary in dioestrus II. Interestingly, the activity of the antioxidants CAT and GPX and lipid peroxide (TBARS) levels varied rhythmically in the mouse ovary in dioestrus, whereas there was no circadian oscillation in antioxidant uric acid levels. This is consistent with previous studies showing that the activity of antioxidant enzymes and lipid peroxidation oscillate rhythmically in several rodent tissues (Ponce *et al.* 2012; Tasaki *et al.* 2013; Navigatore-Fonzo *et al.* 2017). Diurnal maximum antioxidant enzyme activity coincides, as expected, with minimum lipid peroxidation levels. Thus, CAT and GPX generate a more antioxidant cellular environment that precedes the BMAL1 protein peak, favouring endogenous clock activity in terms of predictive homeostasis. In contrast, lipid peroxidation, a marker of cellular oxidative stress, is higher around the middle of the night, probably because of minimal antioxidant enzyme activity at that moment.

It is known that oxidative stress induces apoptosis via the death-receptor pathway Fas/FasL/Fas-associated death domain (FADD) and that an increase in lipid peroxidation (TBARS), in particular, is associated with that type of cell death (Chang *et al.* 2014; Verma *et al.* 2014). Consistent with that, in the present study maximum lipid peroxide levels were found to occur with maximum *Fas* and *FasL* expression in the mouse ovary in dioestrus.

It is known that dioestrus II is the stage when the CL lifespan ends to start a new oestrous cycle. We suggest that the sequence of events described above and summarised in the phase map shown in Fig. 6 (for WT) accounts for a temporal organisation in the ovary that leads to physiological luteal regression. The rhythmic expression and activity of the factors studied herein,

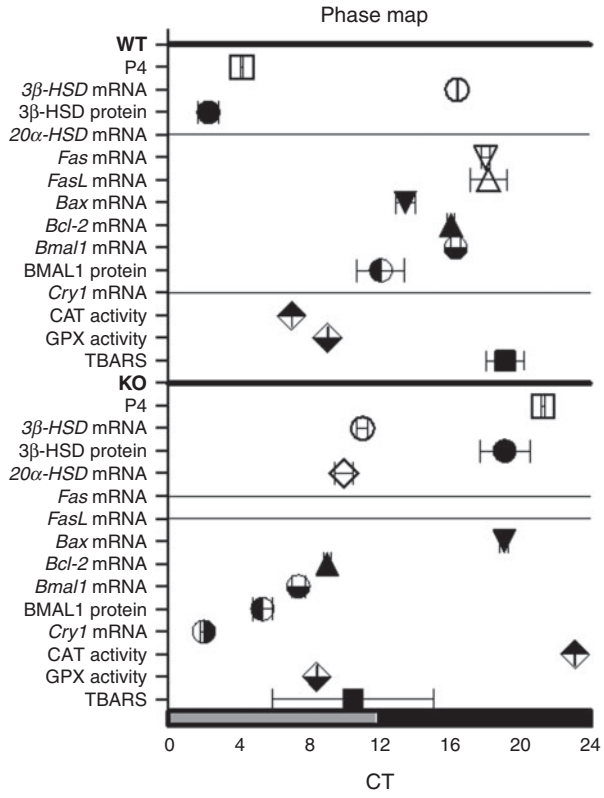

Fig. 6. Phase map of endogenous rhythms showing the temporal distribution of the acrophases of factors involved in functional and structural luteal regression and its putative regulators in the ovary of wild-type (WT) and p55 tumour necrosis factor receptor (TNFRp55)-knockout (KO) mice in dioestrus. The bar on the axis of the abscissa represents the subjective day (grey) and night (black) over a 24-h period. CT, circadian time (where CT0 corresponds to the beginning of the 'subjective day'; that is, when the light went on). HSD, hydroxysteroid dehydrogenase; *FasL*, Fas ligand; *Bmal1*, brain and muscle ARNT-Like protein 1; *Cry1*, cryptochrome 1; CAT, catalase; GPX, glutathione peroxidase; TBARS, thiobarbituric acid-reactive substances.

as well as the presence of putative clock-responsive sites in the regulatory regions of their genes and the order in which the acrophases occur with regard to the BMAL1 protein peak suggest participation of the endogenous clock in the circadian regulation of luteal regression (Fig. 6).

Considerable evidence supports a role for TNF-α in autocrine and paracrine processes central to reproduction, including gamete and follicle development, steroidogenesis, uterine cyclicity, placental differentiation, development of the embryo and parturition (Rojas-Cartagena *et al.* 2005). In addition, it has been demonstrated that: (1) TNF-α has a role in the regulation of the inflammatory process involved in the oestrous cycle (Stocco *et al.* 2007); (2) activation of TNFRp55 primarily leads to proinflammatory and programmed cell death pathways (Terranova *et al.* 1995); and (3) TNFRp55 is involved in the modulation of cellular clock activity in several tissues (Arjona and Sarkar 2006; Cavadini *et al.* 2007). All of these led us to continue investigating the effects of TNFRp55 deficiency on endogenous circadian rhythms of factors related to luteal regression in the ovary during dioestrus.

Of note, as shown in Fig. 6 (for KO), TNFRp55 deficiency alters the temporal organisation in the ovary of mice in dioestrus.

TNFRp55 KO mice show altered circadian patterns of P4 and 3β-HSD expression, as well as rhythmic 20α-HSD expression, in the ovary during dioestrus, probably because of changes in the circadian oscillation of BMAL1 and CRY1. Interestingly, TNFRp55 deficiency reduced P4 rhythmicity and shifted the phase, exhibiting a peak P4 levels towards the end of the day. To the best of our knowledge, there are is no evidence of p55-mediated TNF-α effects on P4 circadian rhythmicity; however, an association between the daily rhythm of TNF-α and diurnal variations in cortisol and prolactin has been reported by Bollinger *et al.* (2010) in a rheumatoid arthritis model. In addition, luteolytic events are induced by TNF-α in the late luteal phase (Okuda and Sakumoto 2003). However, how TNF-α switches from being a luteotrophic to a luteolytic agent in the oestrous cycle is unknown. It has been shown that TNF-α reduces P4 concentrations in the CL of pigs (Endo *et al.* 1998). It is known that P4 acts as a survival factor in several reproductive tissues by altering the expression of anti- and proapoptotic genes of the Bcl-2 family. Candolfi *et al.* (2005) showed that P4 impairs the permissive effect of oestradiol on lactotropes and somatotropes to TNF-α-induced apoptosis. The phase delay of the P4 rhythm in the ovary of TNFRp55-deficient mice may be a cause, or a consequence, of a delay in the beginning of luteal functional regression. Only a few studies have investigated the role of TNFRp55 signalling in P4 metabolism (Abdo *et al.* 2008; Vallcaneras *et al.* 2017), and no one has reported the effects of TNF-α on P4 circadian rhythmicity. The present study is, to the best of our knowledge, the first report on the effects of TNFRp55 deficiency on circadian patterns of steroidogenesis and luteal regression in the ovary.

Abdo *et al.* (2008) suggested the participation of TNF-α, via its p55 receptor, in CL regression in the rat, with decreased StAR expression. Conversely, an increase in 20α-HSD expression and activity has been associated with luteal functional regression (Stocco *et al.* 2007). In the present study, even though TNFRp55 deficiency did not modify *StAR* mRNA levels throughout the day, it made 20α-HSD expression rhythmic, with an acrophase that occurred with the nadir of the rhythm of P4 on the second half of the subjective day. In addition, TNFRp55 deficiency also advanced the acrophase of the *3β-HSD* rhythm but delayed the 3β-HSD protein peak (Figs 1, 6). These results are in agreement with those of Leone *et al.* (2012), who found that intracerebroventricular delivery of TNF-α induced a phase delay of wheel-running activity rhythms, suggesting that the SCN, and subsequently the peripheral clocks, respond to the cytokine *in vivo*. Thus, as expected, TNFRp55 deficiency in the present study advanced the acrophase of the *3β-HSD* mRNA rhythm. Even though some studies have reported that TNF-α downregulates the activity of steroidogenic enzymes during an immune response (Mukhopadhyay *et al.* 2009), this is the first evidence of the participation of TNFRp55 in the circadian regulation of 3β-HSD in the ovary. At this point, we wondered whether such participation could be mediated by the endogenous clock.

It has been demonstrated that TNF-α modulates (attenuate) endogenous clock activity (Cavadini *et al.* 2007; Petrzilka *et al.* 2009). Specifically, Yoshida *et al.* (2013) demonstrated that TNF-α increases *Bmal1* and *Cry1* transcript levels but it has no effect on *Clock* or *Per1* expression. In the present study, TNFRp55 deficiency modified circadian rhythmicity of the endogenous clock factors. Interestingly, we found different effects of TNFRp55 deficiency on the circadian expression of *Bmal1* and *Cry1* in the ovary: Bmal1 mRNA and protein rhythms were significantly phase advanced in KO compared with WT mice, whereas *Cry1* expression turned out to be rhythmic in ovaries of TNFRp55-deficient mice (Figs 4, 6). This could be explained by the findings of Cavadini *et al.* (2007), who demonstrated that TNF-α interferes with E-box-mediated clock transcriptional activation. In contrast, we could suggest that in the absence of TNFRp55 and, consequently, under a deficient TNF-α signalling there would be derepression of BMAL1:CLOCK controlled Cry transcription, leading to rhythmic *Cry1* gene expression observed in the KO mice. Similarly, the phase advance observed in the circadian expression of *Bmal1* could be explained by derepressed transcription of its activator retinoid-related orphan receptor-alpha (Rora). Thus, the results of the present study point to the clock *Bmal1* and *Cry1* genes as transcriptional targets for TNF-α signalling in the ovary.

As expected, changes in the local cellular clock of TNFRp55-KO mouse ovary give rise to temporal changes in the expression of clock-controlled genes, such as the apoptosis-related *Bax*, *Fas*, *FasL* and *Bcl-2* genes. Lack of TNFRp55 delays the occurrence of maximum *Bax* levels, makes *Fas* and *FasL* expression arrhythmic and phase advances the rhythm of anti-apoptotic *Bcl-2*. In addition to the delay in P4 rhythm, these observations could be associated with the delay in luteal regression in TNFRp55-deficient mice.

High levels of TNF-α have been associated with increased levels of oxidative stress in different tissues. Somehow paradoxically, in the present study, TNFRp55 deficiency increased the mesor and amplitude and advanced the acrophase of the lipid peroxidation rhythm in the mouse ovary. In the concept of predictive homeostasis, it is likely that the results obtained tend to protect endogenous clock functioning; the peak in CAT activity was delayed towards the end of the night–beginning of the day and the amplitude of the GPX activity rhythm increased earlier than the lipid peroxidation peak in the ovary of TNFRp55-deficient mice.

The present results strengthen the hypothesis that dysregulation of TNF-α signalling may be the potential cause of altered circadian and menstrual cycling in some gynaecological diseases. The results could explain the infertility-related pathologies suffered by women under clock-related stress, such as chronic jet lag, sleep disorders and shift work. We expect that the data from the present study will highlight endogenous clock and TNFRp55 signalling as potential novel therapeutic targets for steroidogenic deficits in the ovary.

Conflicts of interests

The authors declare no conflict of interest.

Acknowledgements

The authors thank Ana Maria Rastrilla for her help with various aspects of this study, Luis Villegas for technical support and the Immunopathology Laboratory of Multidisciplinary Institute of Biological Research of San Luis (IMIBIO-SL), Argentina, for providing the knockout mice. This work was supported by grants from the National University of San Luis (PROICO 2-1812 and PROICO 2-0010) and the National Scientific and Technical Research Council, Argentina (Grant PIP 2399). This work is part of the doctoral thesis of Magali del Carmen de la Vega.

References

Abdo, M., Hisheh, S., Arfuso, F., and Dharmarajan, A. (2008). The expression of tumor necrosis factor-alpha, its receptors and steroidogenic acute regulatory protein during corpus luteum regression. *Reprod. Biol. Endocrinol.* **6**, 50–61. doi:10.1186/1477-7827-6-50

Aebi, H. (1984). Catalase *in vitro*. *Methods Enzymol.* **105**, 121–126. doi:10.1016/S0076-6879(84)05016-3

Al-Gubory, K. H., Garrel, C., Faure, P., and Sugino, N. (2012). Roles of antioxidant enzymes in corpus luteum rescue from reactive oxygen species-induced oxidative stress. *Reprod. Biomed. Online* **25**, 551–560. doi:10.1016/J.RBMO.2012.08.004

Arjona, A., and Sarkar, D. K. (2006). Evidence supporting a circadian control of natural killer cell function. *Brain Behav. Immun.* **20**, 469–476. doi:10.1016/J.BBI.2005.10.002

Boden, M. J., Varcoe, T. J., Voultsios, A., and Kennaway, D. J. (2010). Reproductive biology of female Bmal1 null mice. *Reproduction* **139**, 1077–1090. doi:10.1530/REP-09-0523

Bollinger, T., Bollinger, A., Naujoks, J., Lange, T., and Solbach, W. (2010). The influence of regulatory T cells and diurnal hormone rhythms on T helper cell activity. *Immunology* **131**, 488–500. doi:10.1111/J.1365-2567.2010.03320.X

Bowen-Shauver, J. M., and Telleria, C. M. (2003). Luteal regression: a redefinition of the terms. *Reprod. Biol. Endocrinol.* **1**, 28. doi:10.1186/1477-7827-1-28

Bussmann, L. E., and Deis, R. P. (1979). Studies concerning the hormonal induction of lactogenesis by prostaglandin F2 in pregnant rats. *J. Steroid Biochem.* **11**, 1485–1489. doi:10.1016/0022-4731(79)90125-0

Candolfi, M., Jaita, G., Zaldivar, V., Zárate, S., Ferrari, L., Pisera, D., Castro, M. G., and Seilicovich, A. (2005). Progesterone antagonizes the permissive action of estradiol on tumor necrosis factor-alpha-induced apoptosis of anterior pituitary cells. *Endocrinology* **146**, 736–743. doi:10.1210/EN.2004-1276

Cartharius, K., Frech, K., Grote, K., Klocke, B., Haltmeier, M., Klingenhoff, A., Frisch, M., Bayerlein, M., and Werner, T. (2005). MatInspector and beyond: promoter analysis based on transcription factor binding sites. *Bioinformatics* **21**, 2933–2942. doi:10.1093/BIOINFORMATICS/BTI473

Cavadini, G., Petrzilka, S., Kohler, P., Jud, C., Tobler, I., Birchler, T., and Fontana, A. (2007). TNF-alpha suppresses the expression of clock genes by interfering with E-box-mediated transcription. *Proc. Natl Acad. Sci. USA* **104**, 12843–12848. doi:10.1073/PNAS.0701466104

Chang, W. T., Hsieh, B. S., Cheng, H. L., Lee, K. T., and Chang, K. L. (2014). Progesterone augments epirubicin-induced apoptosis in HA22T/VGH cells by increasing oxidative stress and upregulating Fas/FasL. *J. Surg. Res.* **188**, 432–441. doi:10.1016/J.JSS.2014.01.063

Chen, H., Zhao, L., Kumazawa, M., Yamauchi, N., Shigeyoshi, Y., Hashimoto, S., and Hattori, M. A. (2013). Downregulation of core clock gene Bmal1 attenuates expression of progesterone and prostaglandin biosynthesis-related genes in rat luteinizing granulosa cells. *Am. J. Physiol. Cell Physiol.* **304**, C1131–C1140. doi:10.1152/AJPCELL.00008.2013

Coogan, A. N., Papachatzaki, M. M., Clemens, C., Baird, A., Donev, R. M., Joosten, J., Zachariou, V., and Thome, J. (2011). Haloperidol alters

circadian clock gene product expression in the mouse brain. *World J. Biol. Psychiatry* **12**, 638–644. doi:10.3109/15622975.2010.543149

Corda, S., Laplace, C., Vicaut, E., and Duranteau, J. (2001). Rapid reactive oxygen species production by mitochondria in endothelial cells exposed to tumor necrosis factor-alpha is mediated by ceramide. *Am. J. Respir. Cell Mol. Biol.* **24**, 762–768. doi:10.1165/AJRCMB.24.6.4228

Davis, J. S., and Rueda, B. R. (2002). The corpus luteum: an ovarian structure with maternal instincts and suicidal tendencies. *Front. Biosci.* **7**, d1949–d1978. doi:10.2741/DAVIS1

Draper, H. H., and Hadley, M. (1990). Malondialdehyde determination as index of lipid peroxidation. *Methods Enzymol.* **186**, 421–431. doi:10.1016/0076-6879(90)86135-I

Endo, T., Henmi, H., Goto, T., Kitajima, Y., Kiya, T., Nishikawa, A., Manase, K., Yamamoto, H., and Kudo, R. (1998). Effects of estradiol and an aromatase inhibitor on progesterone production in human cultured luteal cells. *Gynecol. Endocrinol.* **12**, 29–34. doi:10.3109/09513599809024967

Fahrenkrug, J., Georg, B., Hannibal, J., Hindersson, P., and Gras, S. (2006). Diurnal rhythmicity of the clock genes Per1 and Per2 in the rat ovary. *Endocrinology* **147**, 3769–3776. doi:10.1210/EN.2006-0305

Flohé, L., and Günzler, W. A. (1984). Assays of glutathione peroxidase. *Methods Enzymol.* **105**, 114–120. doi:10.1016/S0076-6879(84)05015-1

Granda, T. G., Liu, X. H., Smaaland, R., Cermakian, N., Filipski, E., Sassone-Corsi, P., and Lévi, F. (2005). Circadian regulation of cell cycle and apoptosis proteins in mouse bone marrow and tumor. *FASEB J.* **19**, 304–306. doi:10.1096/FJ.04-2665FJE

Hardeland, R., Coto-Montes, A., and Poeggeler, B. (2003). Circadian rhythms, oxidative stress, and antioxidative defense mechanisms. *Chronobiol. Int.* **20**, 921–962. doi:10.1081/CBI-120025245

Leone, M. J., Marpegan, L., Duhart, J. M., and Golombek, D. A. (2012). Role of proinflammatory cytokines on lipopolysaccharide-induced phase shifts in locomotor activity circadian rhythm. *Chronobiol. Int.* **29**, 715–723. doi:10.3109/07420528.2012.682681

Lowry, O. H., Rosebrough, N. J., Farr, A. L., and Randall, R. J. (1951). Protein measurement with the Folin phenol reagent. *J. Biol. Chem.* **193**, 265–275.

Mukhopadhyay, R., Mishra, M. K., Basu, A., and Bishayi, B. (2009). Modulation of steroidogenic enzymes in murine lymphoid organs after immune activation. *Immunol. Invest.* **38**, 14–30. doi:10.1080/08820130802480570

Nakamura, T. J., Sellix, M. T., Kudo, T., Nakao, N., Yoshimura, T., Ebihara, S., Colwell, C. S., and Block, G. D. (2010). Influence of the estrous cycle on clock gene expression in reproductive tissues: effects of fluctuating ovarian steroid hormone levels. *Steroids* **75**, 203–212. doi:10.1016/J.STEROIDS.2010.01.007

Nakao, N., Yasuo, S., Nishimura, A., Yamamura, T., Watanabe, T., Anraku, T., Okano, T., Fukada, Y., Sharp, P. J., Ebihara, S., and Yoshimura, T. (2007). Circadian clock gene regulation of steroidogenic acute regulatory protein gene expression in preovulatory ovarian follicles. *Endocrinology* **148**, 3031–3038. doi:10.1210/EN.2007-0044

Navigatore-Fonzo, L., Castro, A., Pignataro, V., Garraza, M., Casais, M., and Anzulovich, A. C. (2017). Daily rhythms of cognition-related factors are modified in an experimental model of Alzheimer's disease. *Brain Res.* **1660**, 27–35. doi:10.1016/J.BRAINRES.2017.01.033

Okuda, K., and Sakumoto, R. (2003). Multiple roles of TNF super family members in corpus luteum function. *Reprod. Biol. Endocrinol.* **1**, 95. doi:10.1186/1477-7827-1-95

Petrzilka, S., Taraborrelli, C., Cavadini, G., Fontana, A., and Birchler, T. (2009). Clock gene modulation by TNF-alpha depends on calcium and p38 MAP kinase signaling. *J. Biol. Rhythms* **24**, 283–294. doi:10.1177/0748730409336579

Ponce, I. T., Rezza, I. G., Delgado, S. M., Navigatore, L. S., Bonomi, M. R., Golini, R. L., Gimenez, M. S., and Anzulovich, A. C. (2012). Daily oscillation of glutathione redox cycle is dampened in the nutritional vitamin A deficiency. *Biol. Rhythm Res.* **43**, 351–372. doi:10.1080/09291016.2011.593847

Pru, J. K., Lynch, M. P., Davis, J. S., and Rueda, B. R. (2003). Signaling mechanisms in tumor necrosis factor alpha-induced death of microvascular endothelial cells of the corpus luteum. *Reprod. Biol. Endocrinol.* **1**, 17. doi:10.1186/1477-7827-1-17

Redlin, U. (2001). Neural basis and biological function of masking by light in mammals: suppression of melatonin and locomotor activity. *Chronobiol. Int.* **18**, 737–758. doi:10.1081/CBI-100107511

Refinetti, R., Corné Lissen, G., and Halberg, F. (2007). Procedures for numerical analysis of circadian rhythms. *Biol. Rhythm Res.* **38**, 275–325. doi:10.1080/09291010600903692

Roby, K. F., Son, D. S., and Terranova, P. F. (1999). Alterations of events related to ovarian function in tumor necrosis factor receptor type I knockout mice. *Biol. Reprod.* **61**, 1616–1621. doi:10.1095/BIOLREPROD61.6.1616

Rojas-Cartagena, C., Appleyard, C. B., Santiago, O. I., and Flores, I. (2005). Experimental intestinal endometriosis is characterized by increased levels of soluble TNFRSF1B and downregulation of Tnfrsf1a and Tnfrsf1b gene expression. *Biol. Reprod.* **73**, 1211–1218. doi:10.1095/BIOLREPROD.105.044131

Sander, V. A., Piehl, L., Facorro, G. B., Rubin de Celis, E., and Motta, A. B. (2008). Regulation of functional and regressing stages of corpus luteum development in mice. Role of reactive oxygen species. *Reprod. Fertil. Dev.* **20**, 760–769. doi:10.1071/RD08051

Sellix, M. T., and Menaker, M. (2011). Circadian clocks in mammalian reproductive physiology: effects of the 'other' biological clock on fertility. *Discov. Med.* **11**, 273–281.

Smith, M. S., Freeman, M. E., and Neill, J. D. (1975). The control of progesterone secretion during the estrous cycle and early pseudopregnancy in the rat: prolactin, gonadotropin and steroid levels associated with rescue of the corpus luteum of pseudopregnancy. *Endocrinology* **96**, 219–226. doi:10.1210/ENDO-96-1-219

Stocco, C., Telleria, C., and Gibori, G. (2007). The molecular control of corpus luteum formation, function, and regression. *Endocr. Rev.* **28**, 117–149. doi:10.1210/ER.2006-0022

Sugino, N., Telleria, C. M., and Gibori, G. (1997). Progesterone inhibits 20alpha-hydroxysteroid dehydrogenase expression in the rat corpus luteum through the glucocorticoid receptor. *Endocrinology* **138**, 4497–4500. doi:10.1210/ENDO.138.10.5572

Tasaki, H., Zhao, L., Isayama, K., Chen, H., Yamauchi, N., Shigeyoshi, Y., Hashimoto, S., and Hattori, M. A. (2013). Profiling of circadian genes expressed in the uterus endometrial stromal cells of pregnant rats as revealed by DNA microarray coupled with RNA interference. *Front. Endocrinol. (Lausanne)* **4**, 82. doi:10.3389/FENDO.2013.00082

Terranova, P. F., and Rice, V. M. (1997). Review: cytokine involvement in ovarian processes. *Am. J. Reprod. Immunol.* **37**, 50–63. doi:10.1111/J.1600-0897.1997.TB00192.X

Terranova, P. F., Hunter, V. J., Roby, K. F., and Hunt, J. S. (1995). Tumor necrosis factor-α in the female reproductive tract. *Proc. Soc. Exp. Biol. Med.* **209**, 325–342. doi:10.3181/00379727-209-43905B

Trinder, P. (1969). Determination of glucose in blood using glucose oxidase with an alternative oxygen acceptor. *Ann. Clin. Biochem.* **6**, 24–27. doi:10.1177/000456326900600108

Vallcaneras, S. S., De la Vega, M., Delgado, S. M., Motta, A., Telleria, C., Rastrilla, A. M., and Casais, M. (2016). Prolactin modulates luteal regression from the coeliac ganglion via the superior ovarian nerve in the late-pregnant rat. *Reprod. Fertil. Dev.* **28**, 565–573. doi:10.1071/RD14184

Vallcaneras, S., Ghersa, F., Bastón, J., Delsouc, M. B., Meresman, G., and Casais, M. (2017). TNFRp55 deficiency promotes the development of

ectopic endometriotic-like lesions in mice. *J. Endocrinol.* **234**, 269–278. doi:10.1530/JOE-17-0236

Verma, D., Hashim, O. H., Jayapalan, J. J., and Subramanian, P. (2014). Effect of melatonin on antioxidant status and circadian activity rhythm during hepatocarcinogenesis in mice. *J. Cancer Res. Ther.* **10**, 1040–1044. doi:10.4103/0973-1482.138227

Welsh, D. K., Takahashi, J. S., and Kay, S. A. (2010). Suprachiasmatic nucleus: cell autonomy and network properties. *Annu. Rev. Physiol.* **72**, 551–577. doi:10.1146/ANNUREV-PHYSIOL-021909-135919

Yoshida, K., Hashiramoto, A., Okano, T., Yamane, T., Shibanuma, N., and Shiozawa, S. (2013). TNF-α modulates expression of the circadian clock gene Per2 in rheumatoid synovial cells. *Scand. J. Rheumatol.* **42**, 276–280. doi:10.3109/03009742.2013.765031

Zhang, Z., Lai, S., Wang, Y., Li, L., Yin, H., Wang, Y., Zhao, X., Li, D., Yang, M., and Zhu, Q. (2017). Rhythmic expression of circadian clock genes in the preovulatory ovarian follicles of the laying hen. *PLoS One* **12**, e0179019. doi:10.1371/JOURNAL.PONE.0179019

Zorov, D. B., Juhaszova, M., and Sollott, S. J. (2006). Mitochondrial ROS-induced ROS release: an update and review. *Biochim. Biophys. Acta* **1757**, 509–517. doi:10.1016/J.BBABIO.2006.04.029

Zuther, P., Gorbey, S., and Lemmer, B. (2009). Chronos-Fit 1.06, http://www.ma.uni-heidelberg.de/inst/phar/lehre/chrono.html [verified 21 March 2017].